High Voltage Gain Dual Active Bridge Converter with an Extended Operation Range for Renewable Energy Systems

Zhang, Zhe; Tomas Manez, Kevin; Xiao, Yudi; Andersen, Michael A. E.

Published in:
Proceedings of 2018 IEEE Applied Power Electronics Conference and Exposition

Link to article, DOI:
10.1109/APEC.2018.8341271

Publication date:
2018

Document Version
Peer reviewed version

High Voltage Gain Dual Active Bridge Converter with an Extended Operation Range for Renewable Energy Systems

Zhe Zhang, Kevin Tomas-Manez, Yudi Xiao and Michael A. E. Andersen
Department of Electrical Engineering
Technical University of Denmark
Kgs. Lyngby, 2800 Denmark
zz@elektro.dtu.dk

***Abstract*—Developing bidirectional dc-dc converters has become a critical research topic and gains more and more attention in recent years due to the extensive applications of smart grids with energy storages, hybrid and electrical vehicles and dc microgrids. In this paper, a Partial Parallel Dual Active Bridge (P^2DAB) converter, i.e. low-voltage (LV) side parallel and high-voltage (HV) side series, is proposed to achieve high voltage gain and low current stress over switching devices and transformer windings. Given the unmodified P^2DAB power stage, by regulating the phase-shift angle between the paralleled active bridges, the power equations and voltage gain are then modified, and therefore the operation range can be extended effectively. The operating principles of the proposed converter and its power characteristics under various operation modes are studied, and the design constraints are discussed. Finally, a laboratory prototype is constructed and tested. Both simulation and experimental results have verified the proposed topology's operation and design.**

Keywords—Bidirectional; converter; DAB; dc-dc; high voltage gain; soft-switching.

I. INTRODUCTION

Bidirectional dc-dc converters provide the capability of effectively and flexibly regulating reversible dc power flows, making them an essential solution in applications such as renewable energy systems, electrical vehicles and dc microgrids [1]-[5]. Several bidirectional dc-dc topologies, as well as their derivations, exist but given the galvanic isolation requirement, the two most established converters are the dual active bridge (DAB) and the isolated boost/buck converter [6], [7]. This paper focuses on the DAB converter, which has been implemented in a wide range of applications including renewable energy conversion, smart transformers, and transportation electrification, due to its unique features such as symmetrical configuration and zero voltage switching (ZVS). However, there are still some fundamental issues existing, for instance, the DAB converter's efficiency suffers from large root mean square (rms) current because of 1) voltage unmatch between low voltage side (LVs) and high voltage side (HVs) and 2) phase-shift control introducing reactive power, and it becomes even severe for high-power applications. Various techniques for high current applications have been proposed. The well-known method is directly parallel semiconductor devices or converter modular units [8]-[11]. Paralleling switches complicates circuit layout and increases parasitic inductance. Moreover, thicker copper or a parallel structure must be applied to transformer windings resulting in high manufacturing cost and high interwinding capacitance, especially for print circuit board (PCB) windings. On the other hand, paralleling converter modular units need additional control scheme to eliminate circulating current between units. Besides paralleling, other methods are targeted towards reactive current reduction and ZVS region extension by using more advanced modulation strategies for instance double- or triple-phase-shift modulations and variable frequency modulations [12]-[14].

In this paper, based on an idea of connecting the circuit parts, which need to carry high current, in parallel and connecting the circuit parts, which need to block high voltage, in series, a new DAB converter configuration, so-called Partial Parallel Dual Active Bridge (P^2DAB) converter is proposed for high-power applications. The ac current balancing between the parallel full-bridges is inherently ensured by the winding series connection on the HVs. Moreover, compared with the traditional DAB converter, regulating the phase-shift angle between the paralleled active bridges gives an additional degree of freedom for power control, and thereby extends the P^2DAB converter's operating range.

II. PROPOSED P^2DAB CONVERTER

The proposed topology is presented in Fig. 1. The converter is derived from a DAB topology with parallel high-current parts. Two transformers operated in parallel on the LVs and in series on the HVs. Due to series connection of the HVs windings, the currents i_1 and i_2 are forced to be the same and can be expressed as,

$$i_1 = i_1 = n \cdot i_{ac} \tag{1}$$

where i_{ac} and n represent the HVs winding current and the transformer turns ratio, respectively, as denoted in Fig. 1.

A single common active full bridge is connected to the high-voltage port V_2. This partial parallel configuration splits the high-current loops into two smaller loops with half the total

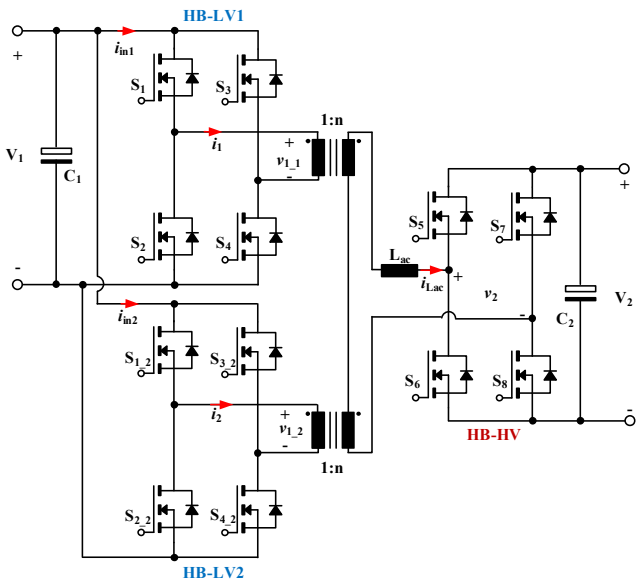

Fig. 1. Topology of the proposed P²DAB.

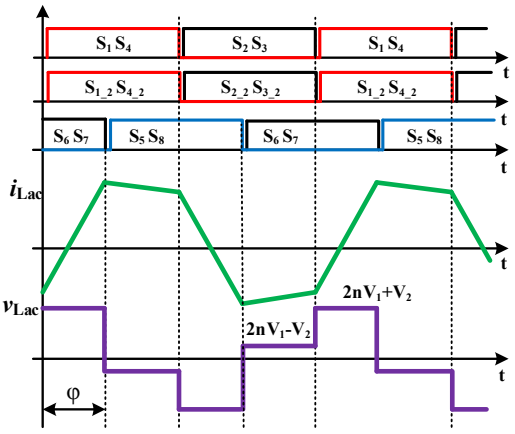

Fig. 2. Basic single phase-shift modulation.

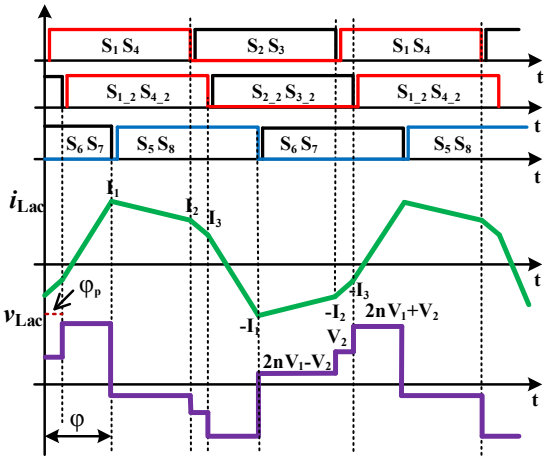

Fig. 3. Phase-shift control of the paralleled active bridges.

input current, and thereby reduces conduction and switching losses. Due to only high-current parts duplicated, cost can be reduced accordingly. The basic converter operating waveforms under single phase-shift modulation are presented in Fig. 2, and the converter's steady-state power equation can be derived from (2).

$$P = \frac{2nV_1V_2}{f_s L_{ac}}\varphi(1-2\varphi) \tag{2}$$

where the phase shift φ is represented as a percentage of the switching period T_s, f_s is the switching frequency and L_{ac} is the sum of the external inductance and the transformer leakage inductance seen from the HVs.

If a fixed load Z_L is connected to V_2 port, the P²DAB converter's voltage gain can be expressed by (3). As it can be observed, it is twice as much as that of conventional DAB converters.

$$G(\varphi) = \frac{V_2}{V_1} = 2n\frac{Z_L}{f_s L_{ac}}\varphi(1-2\varphi). \tag{3}$$

This partial parallel principle can also be applied to other DAB derived topologies, such as single active bridge (SAB), dual half bridge (DHB) and dual three- or multi-phase bridge (DTB or DMB) converters for high-current applications.

III. Operating Range Extension

A. Additional Phase-shift and Effects

Regulating the phase shift between the two paralleled active bridges, i.e. HB-LV1 and HB-LV2 gives an additional degree of freedom to control output power or voltage. Fig. 3 shows the switching pattern and the typical ac inductor current and voltage waveforms when the additional phase shift φ_p is inserted and $0<\varphi_p<\varphi$. Based on the waveforms in Fig. 3, I_1, I_2 and I_3 can be calculated accordingly in (4)-(6). By using the mean-value theorem, the power equation for P²DAB with φ and φ_p as the control parameters is expressed in (7).

$$I_1 = \frac{(4\varphi - 2\varphi_p - 1)\cdot 2nV_1 + V_2}{4 f_s L_{ac}}. \tag{4}$$

$$I_2 = \frac{(1-2\varphi_p)\cdot 2nV_1 + (4\varphi - 1)\cdot V_2}{4 f_s L_{ac}}. \tag{5}$$

$$I_3 = \frac{(1-2\varphi_p)\cdot 2nV_1 + (4\varphi - 4\varphi_p - 1)\cdot V_2}{4 f_s L_{ac}}. \tag{6}$$

$$P = \frac{2nV_1V_2}{f_s L_{ac}}\varphi\left(1 - 2\varphi + 2\varphi_p - \frac{\varphi_p}{2\varphi} - \frac{\varphi_p^2}{\varphi}\right) \quad (0<\varphi_p\leq\varphi). \tag{7}$$

Equation (7), in comparison to (2), has an additional term i.e. $2\varphi_p - \frac{\varphi_p}{2\varphi} - \frac{\varphi_p^2}{\varphi}$ which is always negative when $0<\varphi\leq 0.25$ (the phase-shift angle is limited to be smaller than $\pi/2$).

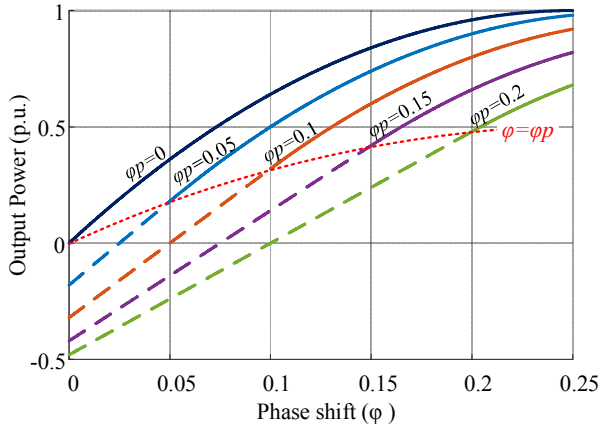

Fig. 4. Power as a function of φ at different φ_p.

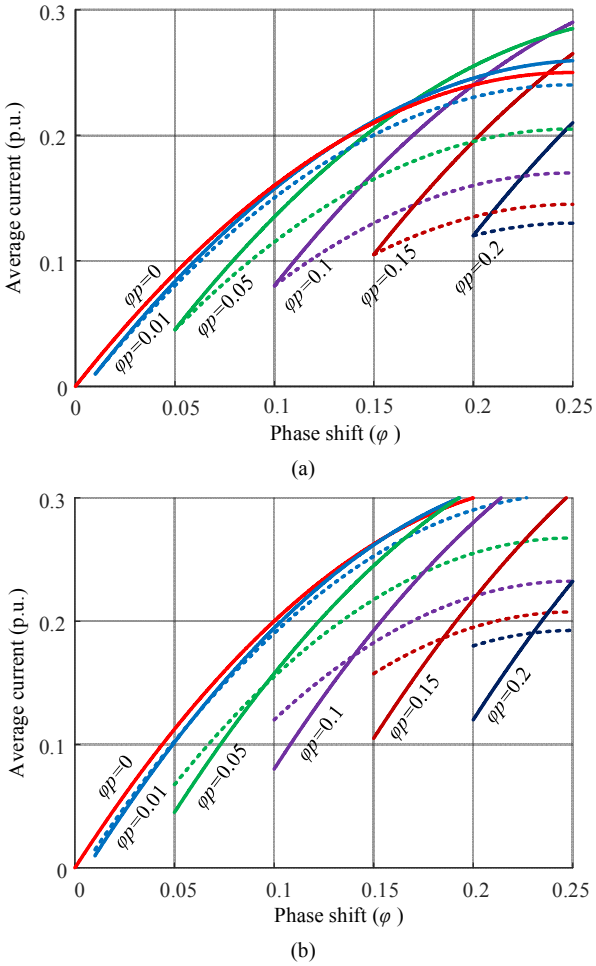

Fig. 5. Average input current as a function of φ_p at different φ. (a) m=1, and (b) $m\neq1$.

Similarly, the power equation for $\varphi<\varphi_p\leq0.25$ is expressed by (8).

$$P=\frac{4nV_1V_2}{f_sL_{ac}}\left(\varphi-\frac{\varphi_p}{2}\right)\left(\frac{1}{2}-\varphi_p\right)\quad(\varphi<\varphi_p\leq0.25). \tag{8}$$

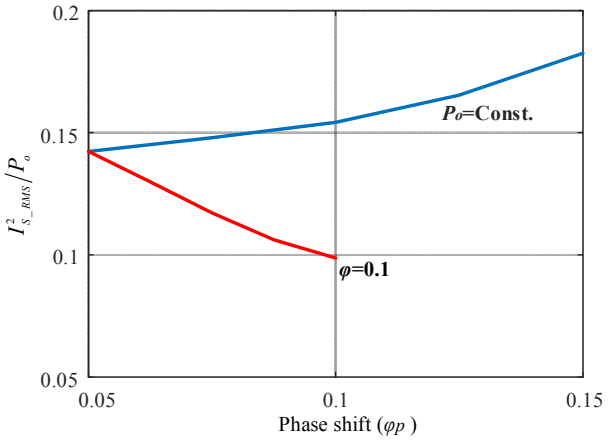

Fig. 6. Variation of rms currents as a function of $\varphi_p<\varphi$.

Therefore, the power as a function of φ and φ_p can be plotted in Fig. 4, where the base power is $nV_1V_2/4f_sL_{ac}$.

B. Design Considerations

It is found that regulating φ_p results in an unequal power distribution between the paralleled active bridges. When $0<\varphi_p<\varphi$, the average input currents I_{in1_avg} and I_{in2_avg} can be calculated by (9) and (10).

$$I_{in1\_avg}=\frac{n^2V_1}{f_sL_{ac}}\left[2m\varphi(1-2\varphi)+\varphi_p(2\varphi_p-1)\right] \tag{9}$$

$$I_{in2\_avg}=\frac{n^2V_1}{f_sL_{ac}}\left[2m(\varphi-\varphi_p)(1-2\varphi+2\varphi_p)+\varphi_p(1-2\varphi_p)\right] \tag{10}$$

where

$$m=\frac{V_2}{2nV_1}. \tag{11}$$

From (9)-(11), it can be seen that the current distribution between the two paralleled bridges depends on the phase-shift angles φ and φ_p and m. When φ_p=0,

$$I_{in1\_avg}=I_{in2\_avg}=\frac{n^2V_1}{f_sL_{ac}}2m\varphi(1-2\varphi)=\frac{nV_2}{f_sL_{ac}}\varphi(1-2\varphi). \tag{12}$$

Fig. 5 shows the ratios of the average currents I_{in1_avg} and I_{in2_avg} against $n^2\cdot V_1/f_s/L_{ac}$ as a function of φ. The dashed line and solid line represent I_{in1_avg} and I_{in2_avg} respectively. When m=1, I_{in1_avg} and I_{in2_avg} always intersect at $\varphi=\varphi_p$. In fact, the introduced φ_p varies the effective phase-shift angle between ac current and voltage, which results in the different input currents. The active bridge in which the ac current and voltage have smaller phase delay will carry more real power and accordingly has larger average input current.

On the other hand, the series winding connection constrains the rms currents to be equal in all the semiconductor switches on the LVs.

$$I_{S1\sim S4\_rms}=I_{S1\_2\sim S4\_2\_rms}. \tag{13}$$

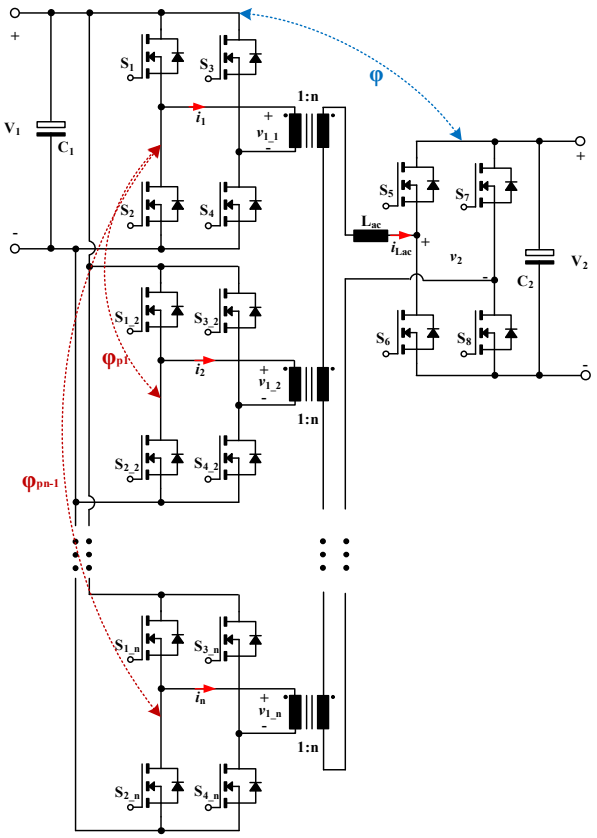

Fig. 7. A high voltage gain DAB converter with multiple partially paralleled LV bridges.

In Fig. 6, $I_{S\_RMS}^2/P_o$ as a function of φ_p is plotted. To keep the output power constant as the blue line illustrated, φ must be increased when increasing φ_p, which leads to higher reactive power as well as a higher rms current. But if φ is fixed, the red line shows that increasing φ_p causes output power reduction, but at the same time, $I_{S\_RMS}^2$ decreases even further so that lowers conduction loss.

For switching losses, S_{1_2}~S_{4_2} have lower turn-off losses than S_1~S_4, since they are turned off at I_3 which is smaller than I_2 at which S_1~S_4 are switched off, as shown in Fig. 3. However, I_2 and I_3 must be positive in order to discharge the MOSFET's output capacitance and achieve ZVS during turn on. The larger the current, the easier the ZVS is achieved.

C. Topological Extension

This partial parallel idea can be extended further and be applied to a DAB converter with multiple transformers in order to carry large current as well as obtain high voltage gain. An example is given in Fig. 6, where the number of branches is n, and accordingly the number of additional and controllable phase-shift angles is n-1.

IV. Experimental Results

The proposed P^{2}DAB converter has been simulated, built and tested to validate the theoretical analysis. The prototype parameters are listed in Table I.

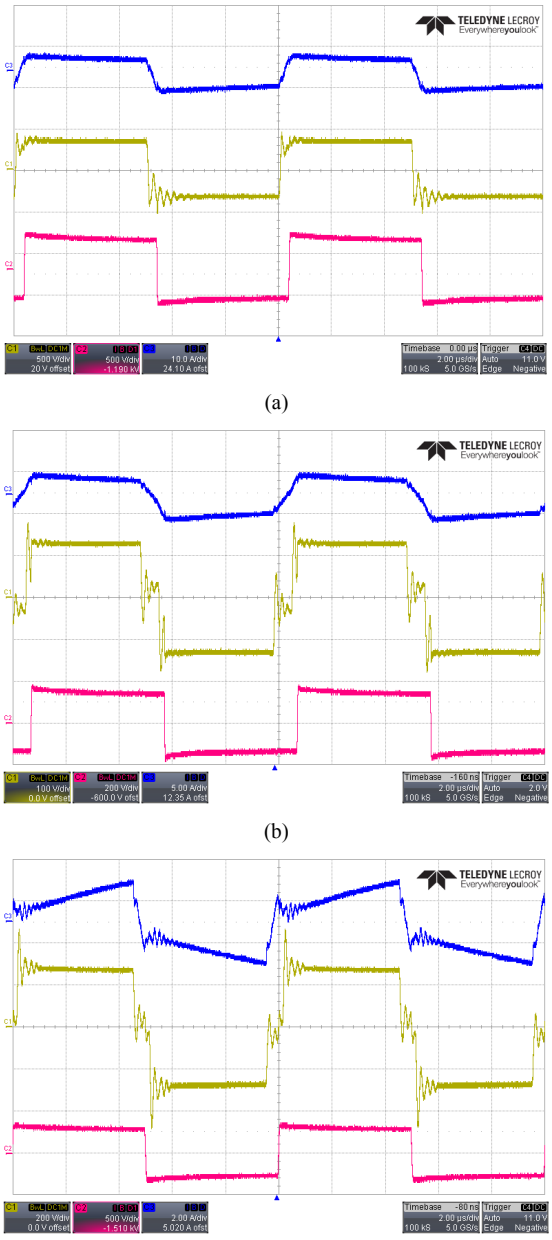

(a)

(b)

(c)

Fig. 8. Experimental waveforms of voltage $n\cdot(v_{1\_1}+v_{1\_2})$ (Ch1), voltage v_2 (Ch2) and current i_{Lac} (Ch3): (a) φ=0.034 and φ_p=0, (b) φ=0.08 and φ_p=0.06, and (c) φ=0.04 and φ_p=0.05. (Time: 2μs/div)

TABLE I. Prototype Parameters

Parameters	Values
V_1 and V_2	50 V and 400 V
Maximum output power, P_{O_max}	1 kW
Transfromers, $Tr1$ and $Tr2$	4:16, 3C90
Inductor, L_{ac}	30 μH
Switching frequency, f_s	100 kHz
Digital controller	TMS320F28335

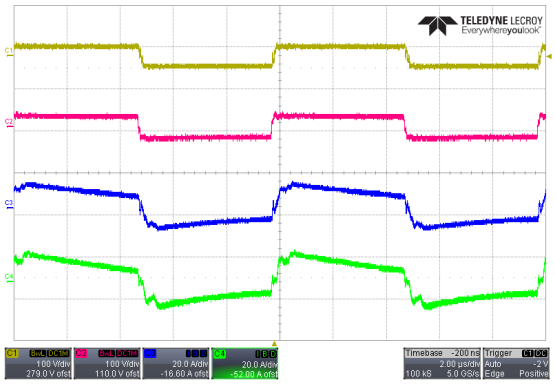

(a)

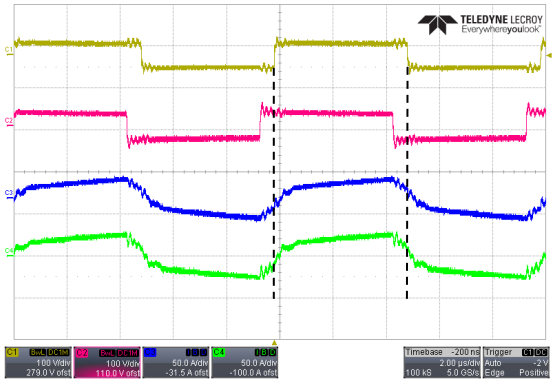

(b)

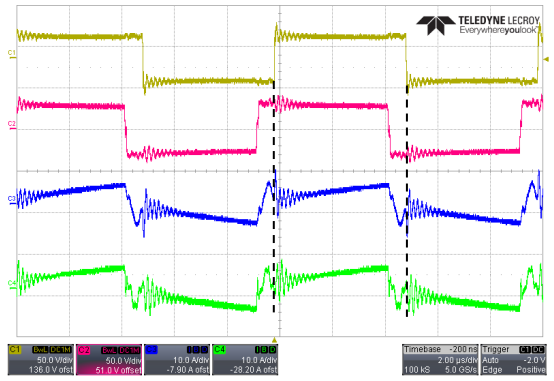

(c)

Fig. 9. Experimental waveforms of voltage v_{1_1} (Ch1), voltage v_{1_2} (Ch2), current i_1 (Ch3) and current i_2 (Ch4): (a) φ_p=0, (b) φ_p<φ, and (c) φ_p>φ (Time: 2μs/div)

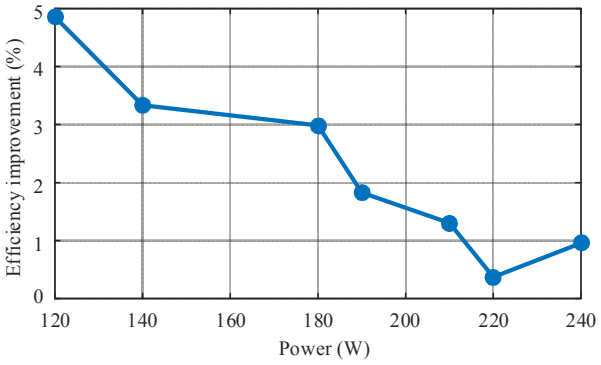

Fig. 10. Measured efficiency improvement at low power.

In Fig. 8, the experimental waveforms with φ_p=0, φ_p<φ and φ_p>φ are presented respectively and the measured results can match the theoretical analysis well. When φ_p≠0, the voltage across the series connected high-voltage windings, i.e. $n\cdot(v_{1\_1}+v_{1\_2})$ becomes a three-level waveform consisting of $\pm 2nV_1$ and 0, which changes the current waveforms accordingly.

The low-voltage side waveforms are given in Fig. 9 to show the effect of φ_p. The currents i_1 and i_2 are always the same regardless the phase-shift angles. Moreover, as it can be observed, L_{ac} makes the ac current lagging behind the ac voltage, which introduces reactive power and leads to extra conduction losses. The larger the phase shift, the higher the loss is. However, regulating φ_p is able to delay the ac voltage v_{1_1}, so that the effective phase-shift angle between v_{1_1} and i_1 is reduced, as highlighted in Fig. 9 (b) and (c) with the dashed lines, and the reactive power decreases. It also explains the reason why the input currents i_{in1} and i_{in2} have different average values.

According to the principles explained above, at the same input and output voltages, using both φ and φ_p to regulate power can improve the converter efficiency at light loads in comparison to the single phase-shift modulation. The measured efficiency improvement is presented in Fig. 10.

V. Conclusion

A new way to extend power level of DAB converters for high-power high-gain applications is proposed and presented in this paper. Partially paralleling allows efficient operation due to small ac loops, reduced current switching losses and fewer high-voltage power devices. Regulating the phase shift between the paralleled active bridges can not only improve the power controllability but also reduce the high-frequency reactive power and, therefore, is more power efficient than the traditional DAB converters with a single phase-shift control.

References

[1] F. Blaabjerg, Z. Chen and S. B. Kjaer, "Power Electronics as Efficient Interface in Dispersed Power Generation Systems," *IEEE Trans. Power Electron.*, vol. 19, no. 5, pp. 1184 - 1194, 2004.

[2] Z. Chen, J. M. Guerrero and F. Blaabjerg, "A Review of the State of the Art of Power Electronics for Wind Turbines," *IEEE Trans. Power Electron.*, vol. 24, no. 8, pp. 1859 - 1875, 2009.

[3] Z. Zhang, R. Pittini, M. A. E. Andersen and O. C. Thomsen, "A Review and Design of Power Electroncis Converters for Fuel Cell Hybrid System Applicaions," *Energy Procedia,* vol. 20, pp. 301-310, 2012.

[4] W. Zhang, D. Xu, X. Li, R. Xie, H. Li, D. Dong, C. Sun and M. Chen, "Seamless Transfer Control Strategy for Fuel Cell Uninterruptible Power Supply System," *IEEE Trans. Power Electron.,* vol. 28, no. 2, pp. 717 - 729, 2013.

[5] Z. Zhang, O. C. Thomsen and M. A. E. Andersen, "Optimal design of a push-pull-forward half-bridge (PPFHB) bidirectional dc–dc converter with variable input voltage," *IEEE Trans. Ind. Electron.*, vol. 59, no. 7, pp.2761-2771, Jul. 2012.

[6] R. W. De Doncker, D. M. Divan, and M. H. Kheraluwala, "A three-phase soft-switched high-power density dc/dc converter for high power applications," *IEEE Trans. Ind. Appl.*, vol. 27, no. 1, pp.63-67, 1991.

[7] R. Pittini, Z. Zhang and Michael A. E. Andersen, "Isolated full bridge boost dc-dc converter designed for bidirectional operation of fuel

cells/electrolyzer cells in grid-tie applications," the *proc. EPE-ECCE Europe*, 2013.

[8] H. Akagi, S. Kinouchi, and Y. Miyazaki, "Bidirectional isolated dual-active-bridge (DAB) DC-DC converters using 1.2-kV 400-A SiC-MOSFET dual modules", *CPSS Trans. Power Electron.* vol. 1, no.1, Dec. 2016.

[9] H. Li, S. M. Nielsen, etc., "Influences of device and circuit mismatches on paralleling silicon carbide MOSFETs," *IEEE Trans. Power Electron.*, vol.31, no.1, Jan. 2016.

[10] M. Liserre, M. Andersen, L. Costa and G. Buticchi, "Power routing in modular smart transformers: active thermal control through uneven loading of cells," *IEEE Ind. Electron. Mag.* vol. 10, no.3, 2016.

[11] G. Buticchi, M. Andresen, M. Wutti and M. Liserre, "Lifetime-based power routing of a quadruple active bridge DC/DC converter," *IEEE Trans. Power Electron.*, vol.32, no.11, Nov. 2017.

[12] G. G. Oggier, G. O. Garcia and A. R. Oliva, "Switching control strategy to minimize dual active bridge converter losses," *IEEE Trans. Power Electron.* , vol.24, no.7, pp.1826-1838, July 2009.

[13] J. Hiltunen, V. Vaisanen, R. Juntunen and P. Silventoinen, "Variable-frequency phase shift modulation of a dual active bridge converter," *IEEE Trans. Power Electron.,* vol.30, no.12, Dec. 2015.

[14] K. L. Jørgensen, M. C. Mira, Z. Zhang and M. A. E. Andersen, "Review of high efficiency bidirectional dc-dc topologies with high voltage gain," the *proc. IEEE 52nd International Universities' Power Engineering Conference*, Jun. 2017.